Cancer Chemother Pharmacol (1999) 44: 65–73

ORIGINAL ARTICLE

Ruediger Port · Friedrich Hanisch · Markus Becker
Peter Bachert · Jens Zeller

Local disposition kinetics of floxuridine after intratumoral and subcutaneous injection as monitored by [^{19}F]-nuclear magnetic resonance spectroscopy in vivo

Received: 7 August 1998 / Accepted: 17 December 1998

Abstract *Purpose*: To test the utility of [^{19}F]-nuclear magnetic resonance (NMR) spectroscopy for studying the kinetics of local drug disposition after interstitial application in vivo. *Methods*: Floxuridine at 30 μmol (2.5% of the reported i.p. 50% lethal dose, LD_{50}) was injected into rats either intratumorally (Morris hepatoma M3924A) or s.c. [^{19}F]-NMR spectra were obtained at the site of administration for up to 5 h after injection using a 2-cm diameter surface coil at 2.0 T. Signal-time data obtained for floxuridine and the metabolite 5-fluorouracil were analyzed using linear compartment models. *Results*: The lower limit for the quantitation of drug remaining at the site of administration was 1 μmol for tumors and 0.2 μmol for the s.c. injection site. Local drug disposition was biexponential in four of six tumors where the half-lives of the fast and slow components of disposition ranged from 4 to 26 and from 33 to 289 min, respectively. It was monoexponential in the remaining two tumors (half-lives 49 and 128 min) and in the s.c. injection experiments ($n = 4$, half-life 6–9 min). 5-Fluorouracil could be quantitated in three of six tumors; the estimated fraction of floxuridine converted intratumorally into 5-fluorouracil was 11–23%. α-Fluoro-β-alanine was detected in the sum spectra of three of the six tumours. *Conclusions*: Local drug-disposition kinetics after interstitial application can be monitored noninvasively by in vivo [^{19}F]-NMR spectroscopy. Disposition kinetics after local injection is highly variable and has a slow component in this tumor, whereas it is much less variable and relatively fast in subcutaneous tissue. The results suggest that NMR spectroscopy may be useful for in vivo studies of drug release from depot preparations designed for interstitial application.

Key words Floxuridine, FUDR · [^{19}F]-NMR spectroscopy in vivo · Tissue pharmacokinetics · Interstitial application

This study was supported by the Deutsche Krebshilfe grant 10-0962-Po 2

R.E. Port (✉)
D-0200, German Cancer Research Center,
P.O. Box 10 19 49, D-69009 Heidelberg, Germany
Tel.: +49-6221-42-3385, Fax: +49-6221-42-3382
e-mail: r.port@dkfz-heidelberg.de

R.E. Port · W.J. Zeller
German Cancer Research Center,
Diagnostics and Experimental Therapy,
Heidelberg, Germany

F. Hanisch · M. Becker · P. Bachert
German Cancer Research Center,
Radiological Diagnostics and Therapy,
Heidelberg, Germany

Introduction

Intratumoral administration of chemotherapeutic agents has successfully been applied to a variety of malignant tumors in experimental animals and in patients as a means of maximizing the antitumor effect while minimizing systemic exposure [12, 19, 24, 27–29, 35, 41, 47, 49, 50]. Intratumoral injection of ethanol into small, single hepatocellular carcinoma nodules appears to be as effective as surgical treatment [6]. Controlled-release preparations have been therapeutically superior to solutions in several of these applications [12, 27, 35, 47], suggesting that local pharmacokinetics has a major impact.

The results of extensive studies of tumor physiology indicate that pharmacokinetics at the tissue level is a crucial problem in the pharmacotherapy of cancer; especially abnormal vascularization and a lack of transport by convection limit the extent of intratumoral drug distribution [21, 22]. To our knowledge, only one study of the local pharmacokinetics of a model compound upon intratumoral injection has been reported [46]; phenol red was injected into a tissue-isolated preparation of the Walker 256 carcinoma in rats and its concentration was monitored in venous outflow during constant rate perfusion. The elimination kinetics of the indicator from tumor was biphasic linear, which was

interpreted as indicating both a well-vascularized and a poorly vascularized compartment of drug distribution.

Nuclear magnetic resonance (NMR) spectroscopy in vivo is a unique tool for the study of pharmacokinetics at the tissue level in that it allows one to monitor concentration changes of drugs and metabolites noninvasively without the need for radioactive labeling. Many studies have demonstrated its applicability in monitoring the pharmacokinetics of drugs in tissues in experimental animals and in patients (for reviews see [4, 32, 33, 40]). 5-Fluorouracil (FU) has been investigated most extensively in vivo [15], but the list of drugs monitored in vivo by NMR spectroscopy includes the anticancer agents gemcitabine [26], iproplatin [20], temozolomide [2], ifosfamide [17, 43], glucosylifosfamide mustard [17], and carboplatin [8] and the experimental antifolate CB3988 [39] as well as fluorine-containing psychotropic drugs [5], lithium [16, 25, 45], the fluorine-containing anesthetic isoflurane [30, 31], and the fluorine-containing antibiotic fleroxacin [23]. Even selective [^{19}F]-NMR imaging of FU and its main catabolite α-fluoro-β-alanine (FBAL) [10] and dynamic imaging of the antifolate CB3988 [34] and of FBAL [4] have been possible in vivo.

The purpose of the present work was to explore the potential of in vivo [^{19}F]-NMR spectroscopy in monitoring local drug-disposition kinetics after interstitial application and to compare the disposition kinetics in tumors with those in s.c. tissue. Fluorine-containing compounds are particularly attractive for this purpose because the sensitivity of ^{19}F is almost as high as that of ^{1}H (the maximal sensitivity attainable except for that of ^{3}H) and because there is no background signal from endogenous compounds. Floxuridine (5-fluoro-2′-deoxyuridine, FUDR) was chosen for study because this highly water-soluble compound may be incorporated into depot preparations at high concentrations and then be used to study retarded-release effects by NMR in vivo.

Materials and methods

Animals, tumors, and drug administration

Female ACI rats purchased from Harlan-Winkelmann (Borchen, Germany) were kept at two per cage under climatized conditions and were given standard food pellets (Altromin) and water ad libitum. Animals were 15–21 weeks old and weighed 170–200 g at the time of the NMR spectroscopy experiments.

Morris hepatoma 3924A cells stored in liquid nitrogen were thawed and were passaged once i.p. Tumor cell ascites was then transplanted s.c. by injection of ca. 5×10^6 cells (0.2–0.4 ml) on the lateral side of the right lower leg. NMR spectroscopy experiments were carried out at 3–7 weeks after s.c. tumor transplantation, when tumors had a maximal diameter of approximately 2.5 cm and weighed 4–6 g. Tumors dissected after the experiment were macroscopically free of necroses.

Floxuridine was kindly supplied by Hoffmann-La Roche AG, Basel, Switzerland. A 0.1-ml aliquot of a 300 m*M* solution in pyrogen-free water for injection (Ampuwa) was injected within 3 s either in the center of the tumor ($n = 6$) or s.c. in the center line of the back of the neck immediately cranially of the scapulae ($n = 4$). The injection needle was left in place for 30 s after the injection to avoid reflux of the injected solution.

NMR measurements

[^{19}F]-NMR experiments were performed at $B_0 = 2.0$ T in a 31-cm-diameter horizontal-bore spectrometer (SIS 85/310; VARIAN, Palo Alto, USA). A home-built 2-cm-diameter planar surface coil (tunable to ^{1}H and ^{19}F Larmor frequencies, 85.52 and 80.46 MHz, respectively) was used in all experiments. The ^{19}F spin-lattice relaxation time (T_1) of floxuridine was 3.5 ± 0.1 s at 2.0 T and 23 °C as measured in an inversion recovery experiment using 0.5 ml of a 100-m*M* model solution of floxuridine in water.

Rats were anesthetized by inhalation of an N_2O/O_2 mixture (40/60, v/v) with added 2% halothane, which was reduced to 0.7% for maintenance. The surface coil was positioned either on the tumor or, in the s.c. injection experiments, in the back of the neck. A 5-mm NMR tube containing 13 μmol of the external standard 1,3-difluoro-2-propanol [DFP, chemical shift (δ) = −158.5 ppm] in a volume of 5 μl was attached to the surface coil. This compound was preferred over trifluoroacetic acid (TFA, $\delta = 0$), which resonates near the halothane spectral region.

After shimming on the tissue ^{1}H water resonance the drug was injected and [^{19}F]-NMR spectra were obtained using a one-pulse-acquire sequence with a 15-μs hard pulse and an acquisition time of 10.4 ms matching the T_2^* decay of the FID. A total of 1,664 complex data points were accumulated over an 80-kHz spectral window. A large number of excitations (NEX) and a short repetition time (T_R) relative to T_1 were used to optimize S/N per unit of time. For animals 1–5 the first n spectra (n between 32 and 152, depending on the S/N) were obtained with NEX = 2,048, followed by spectra recorded with NEX = 16,384; for animals 6–10, NEX = 8,192 was used throughout. The repetition time was $T_R = 22$ ms for animals 1–3 and was changed to $T_R = 16.5$ ms in the other animals subsequent to a hardware upgrade.

All FIDs were zero-filled to 8k data points and multiplied by an exponential function for line-broadening ($\tau^{-1} = 100$ Hz) before Fourier transformation and phase correction. After baseline correction the spectra were analyzed using a least-squares-fit routine (VNMR, VARIAN) assuming Lorentzian line shapes of the resonances. For kinetic analysis, every eight short spectra (NEX = 2,048) of animals 1–5 were added. The temporal resolution of the final signal-time data as used for kinetic analysis was 6.0 (animals 1–3), 4.5 (animals 4 and 5), and 2.25 min (animals 6–10), respectively.

Kinetic analysis

A linear three-compartment model (Fig. 1) was used to describe the floxuridine and FU signal-time data. It is assumed that a fraction $D \cdot (1 - sl)$ of drug input enters a rapidly eliminating compartment, whereas the remainder ($D \cdot sl$) enters a compartment with slow elimination (D Dose, sl fraction of the dose going into the slowly eliminating compartment). The measured floxuridine signal is assumed to be the sum of the signals from these two compartments. FU, where measurable, is assumed to be formed from both floxuridine compartments at the same rate (k_{x3}) and to have a uniform elimination rate constant (k_{30}), independently of the site of formation. The model equation for the floxuridine signal versus time is

$$S = D \cdot sf \cdot [(1 - sl) \cdot e^{-\lambda_1 \cdot t} + sl \cdot e^{-\lambda_2 \cdot t}], \quad (1)$$

where S is the measured [^{19}F]-NMR signal intensity, t is the time after injection, sf is a scaling factor relating the extrapolated signal intensity at $t = 0$ to the applied dose (unit: μmol^{-1}), λ_1 is the sum of the exit rate constants from the rapidly eliminating floxuridine compartment ($\lambda_1 = k_{10} + k_{x3}$, where k_{10} describes the elimination of floxuridine into the circulating blood), and λ_2 is the sum of the corresponding exit rate constants, k_{20} and k_{x3}, for the slowly eliminating floxuridine compartment; sl was fixed to 1 for those

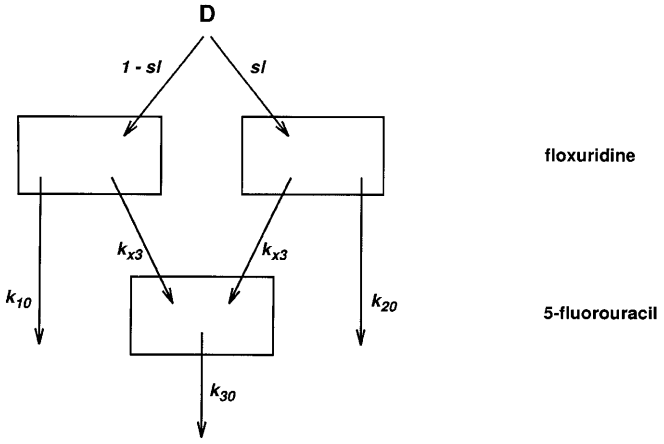

Fig. 1 Linear three-compartment model for analysis of local floxuridine disposition after intratumoral bolus injection. Part of the injected drug ($D \cdot sl$) enters a "slow" compartment, from which it is eliminated unchanged at rate constant k_{20}; the remainder [$D \cdot (1 - sl)$] enters a fast compartment with an elimination rate constant of k_{10}. 5-Fluorouracil (FU) is formed from both floxuridine compartments at the same rate, k_{x3}; its own elimination rate constant is k_{30}. The measured floxuridine signal is assumed to be the sum of the signals from both floxuridine compartments; k_{x3} is set to zero for experiments where FU signals are not present or are too low for quantitation, and sl is set to 1 for tumors with monoexponential disposition of floxuridine and is set to zero for s.c. injection experiments

tumors where floxuridine disposition was monoexponential, whereas it was fixed to 0 for the s.c. injection experiments. The model equation for the FU signal versus time can be derived by the application of Laplace transformations and the partial fractions theorem [9], the result being:

$$S = D \cdot sf \cdot 0.74 \cdot k_{x3} \cdot \left[(1 - sl) \cdot \frac{e^{-k_{30} \cdot t} - e^{-\lambda_1 \cdot t}}{\lambda_1 - k_{30}} + sl \cdot \frac{e^{-k_{30} \cdot t} - e^{-\lambda_2 \cdot t}}{\lambda_2 - k_{30}} \right]. \quad (2)$$

The factor 0.74 is the ratio of the FU and floxuridine signal intensities recorded for equimolar amounts of both compounds (10-mM model solution in HEPES buffer at pH 7.4) as determined with the NMR pulse sequence used in the in vivo experiments. In the absence of experimental data it was assumed to be the same in vivo.

Residual variability was modeled according to

$$y_{\text{observed},i} = y_{\text{predicted},i} + y^{\theta}_{\text{predicted},i} \cdot \varepsilon_i, \quad (3)$$

where $i = 1, \ldots$, the total number of measurements in each animal, ε is normally distributed with mean zero and variance σ^2, and θ is a "turning parameter" describing the degree of heteroscedasticity; θ was set to 0.5 (increasing coefficient of variation with decreasing signal) for all experiments.

The mean residence time (MRT) of floxuridine was calculated using the equation:

$$MRT = \frac{1}{\lambda} \quad (4)$$

for monoexponential fits and

$$MRT = \frac{(1 - sl)}{\lambda_1} + \frac{sl}{\lambda_2} \quad (5)$$

for biexponential fits. Note that Eq. 5 differs from the more commonly used expression $MRT = \int_0^\infty t \cdot C \cdot \mathrm{d}t / \left[\int_0^\infty C \cdot \mathrm{d}t\right]$ [also denoted by $AUMC/AUC$ (area under the first moment curve/area under the curve)]. The $AUMC/AUC$ formula requires that drug elimination be related to the observed concentration by the same constant of proportionality at all times [44]. It is valid, for example, for mammillary models where elimination occurs exclusively from the central compartment [37]. In contrast, the model of Fig. 1 and Eq. 1 implies the assumption that the observed signal is the sum of the signals from two compartments with different exit rates such that the ratio of the observed signal and the rate of elimination from the system varies with time. An expression analogous to Eq. 5 has been used to define the mean residence time of a metabolite formed after peroral drug intake during and after the first pass through the liver [11].

The total amount of FU generated from floxuridine is k_{x3} times the amount of floxuridine, integrated from $t = 0$ to $t = \infty$:

Fig. 2 Representative in vivo [^{19}F]-NMR spectrum obtained at 1 h 40 min after intratumoral injection of 30 μmol floxuridine (animal 5). The measurement time was 4.5 min (TR = 16.5 ms, NEX = 16384). Assignments of resonances, *from left to right*, include trifluoroacetic acid (TFA, metabolite of the anesthetic, $\delta = 0$ ppm), halothane (inhalation anesthetic, −7 ppm), floxuridine (−90 ppm), 5-fluorouracil (−94 ppm), and 1,3-difluoro-2-propanol (DFP, standard, −158 ppm). Possible peaks outside the range from −89 to −126 ppm, other than those of TFA, halothane, and DFP, were not consistently observed and cannot be attributed to known metabolites of floxuridine or FU [4]

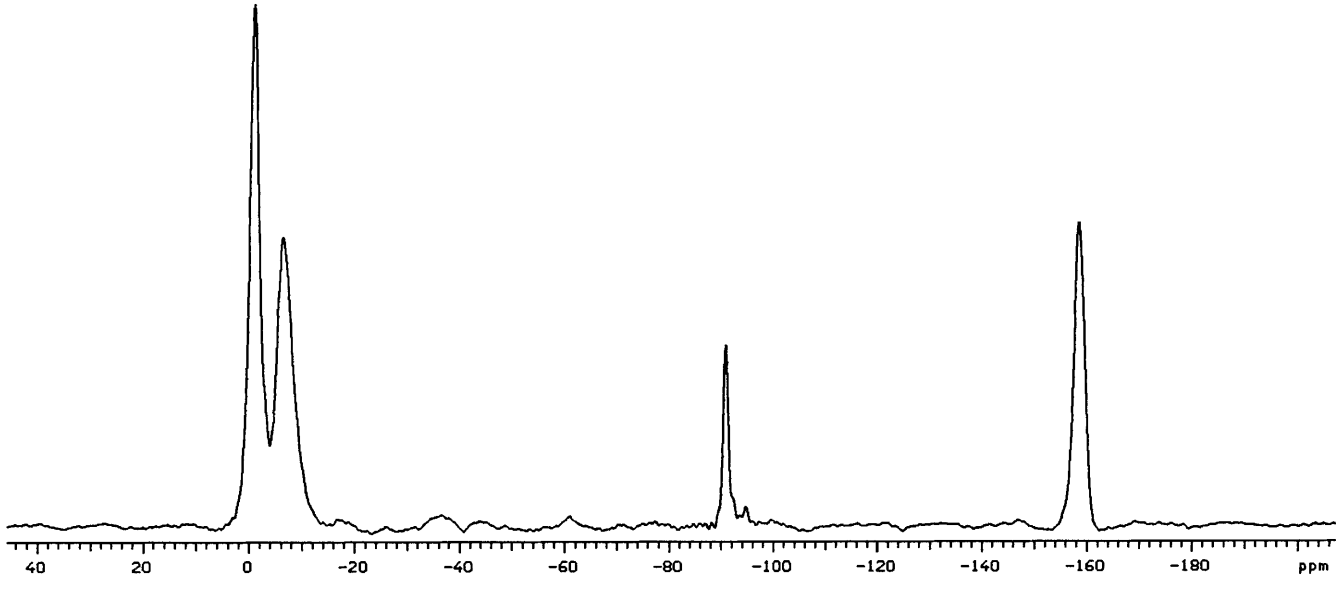

$$A_{FU,\text{total}} = \int_0^\infty k_{x3} \cdot D \cdot [(1 - sl) \cdot e^{-\lambda_1 \cdot t} + sl \cdot e^{-\lambda_2 \cdot t}] \cdot dt$$
$$= k_{x3} \cdot D \cdot \left(\frac{1 - sl}{\lambda_1} + \frac{sl}{\lambda_2}\right),$$

which, upon substitution of Eq. 5, becomes

$$A_{FU,\text{total}} = k_{x3} \cdot D \cdot MRT. \quad (6)$$

The program system NONMEM, version IV [7], was used for model fitting, and the program system S-Plus [48] was used for graphic and statistical analysis.

Results

A representative [^{19}F]-NMR spectrum obtained in vivo is shown in Fig. 2. The signals in the center ($\delta = -90$ and -94 ppm, respectively) are from the injected drug floxuridine and its metabolite FU; the stronger signals on the far left and far right are from the inhalation anesthetic halothane and the standard DFP, respectively. The line widths of floxuridine and the standard DFP were 65 and 165 Hz, respectively. Sum spectra were obtained at 3–4 h after injection to check for the presence of FU nucleotide signals; an example is shown in Fig. 3.

A weak FU resonance at $\delta = -94.3$ ppm appeared in four of six tumors at about 5 min after injection. The FU signal-to-noise ratio (S/N) was generally close to the quantitation limit of S/N = 3. The sum of all spectra with NEX = 16,384 in three of six tumors (tumors 1, 3, and 4) exhibited a weak and broad resonance at $\delta = -112.7$, assigned to α-fluoro-β-alanine (FBAL). No FU nucleotide signal was resolved in any of the spectra, including sum spectra obtained at 3–4 h after injection (Fig. 3).

The signal-time data for floxuridine could be satisfactorily described by the model depicted in Fig. 1 with either one or two distribution compartments. Coefficients of variation (CV) of parameter estimates were less than 10%, except for λ_2 in experiment 3 and k_{30} in experiments 1 and 4, where the CV ranged between 10% and 20%.

The disposition of floxuridine was biexponential in four of six tumors (Fig. 4, tumors 1, 3, 4, and 6). The half-lives of the fast and slow components of disposition ranged from 4 to 26 min and from 33 to 289 min, re-

Fig. 3 In vivo [^{19}F]-NMR spectrum (sum of ten 6-min spectra) obtained at 3–4 h after the intratumoral injection of 30 μmol floxuridine (animal 3), showing floxuridine ($\delta = -90$ ppm) and FU ($\delta = -94$ ppm) resonances

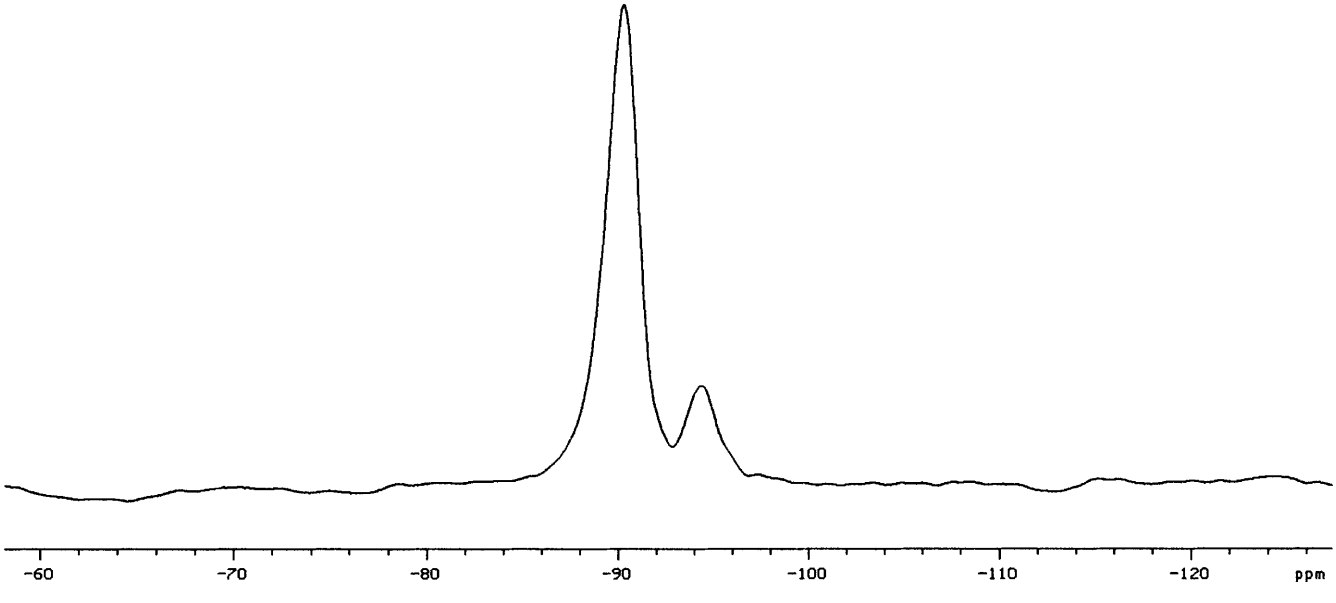

Fig. 4 In vivo [^{19}F]-NMR signal intensity (logarithmic scale) plotted versus time after the injection of 30 μmol floxuridine, by experiment (*Black symbols* Floxuridine, *white symbols* FU, *right ordinate* estimated amount [μmol] of the parent drug remaining at the injection site)

Table 1 Parameters of floxuridine local disposition kinetics after intratumoral and s.c. injection (*i.t.* Intratumoral injection; *s.c.* subcutaneous injection; *sf* scaling factor; *sl* fraction of the dose going into the slowly eliminating compartment; $t_{1/2,1}$, $t_{1/2,2}$ elimination half-lives of the fast and slow compartments, respectively; *FU/D* fraction of floxuridine converted into 5-FU; $t_{1/2,FU}$ elimination half-life of 5-FU)

Animal	Route of admin.	*sf* (μmol^{-1})	*sl*	$t_{1/2,1}$ (min)	$t_{1/2,2}$ (min)	FU/D	$t_{1/2,FU}$ (min)
1	i.t.	2.54	22%	17	190	14%	307
2	i.t.	4.04			49		
3	i.t.	2.67	22%	26	289		
4	i.t.	2.31	44%	8.0	126	11%	188
5	i.t.	3.56			128	23%	103
6	i.t.	2.84	19%	3.9	33		
7	s.c.	17.2		9.1			
8	s.c.	23.3		6.0			
9	s.c.	12.9		8.2			
10	s.c.	14.5		7.7			

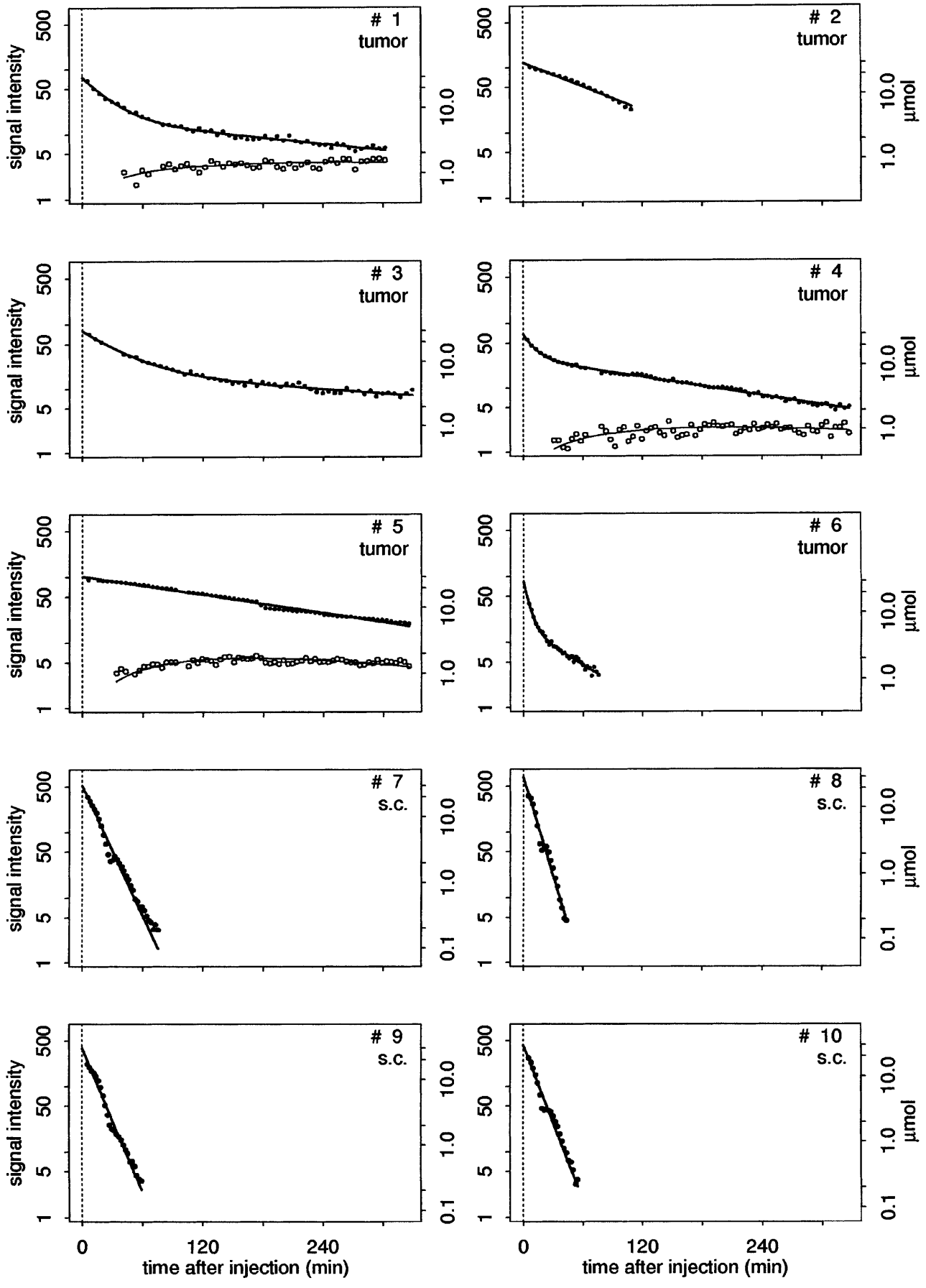
1
tumor
2
tumor
3
tumor
4
tumor
5
tumor
6
tumor
7
s.c.
8
s.c.
9
s.c.
10
s.c.
signal intensity
1
5
50
500
µmol
0.1
1.0
10.0
0
120
240
time after injection (min)

spectively (Table 1). The slow component accounted for 14–40% of the total area under the signal-time curve. One tumor showed monoexponential drug disposition with a half-life of 128 min (Fig. 4, tumor 5). Drug disposition also appeared to be monoexponential with $t_{1/2}$ = 49 min in another tumor (Fig. 4, tumor 2) where NMR monitoring, due to technical problems, was limited to 2 h after injection. FU was detectable in four tumors (tumors 1, 3, 4, and 5), and its kinetics was evaluable in three cases (tumors 1, 4, and 5; Fig. 4); the estimated fraction of the dose of floxuridine converted into FU ranged from 11% to 23%, and the estimated half-life of FU elimination ranged from 103 to 307 min (Table 1).

Local drug disposition was monoexponential after s.c. injection with half-lives ranging from 6 to 9 min (Fig. 4, Table 1). The scale parameters relating the signal intensity to the local amount of drug were almost 1 order of magnitude higher for the s.c. injection site as compared with the tumor (Table 1), resulting in a lower limit of quantitation of 0.2 μmol (Fig. 4, right *y*-scales). No floxuridine metabolite was detected in the experiments involving s.c. injection.

The estimated MRT of drug at the site of measurement was generally much longer in tumors than in s.c. tissue (Fig. 5). The coefficient of interindividual variation of the MRT was 62% for tumor versus 17% for s.c. tissue.

A downward "blip" of the floxuridine signal was consistently observed in the s.c. injection experiments within 15–30 min of injection (Fig. 4). A plot of residuals from the fitted monoexponential disposition curve (observed – predicted signal intensity) versus the time after injection (Fig. 6) reveals an oscillation of observed signal intensity about the predicted disposition curve, which could be an indication of lateral drug movement in loose s.c. connective tissue through regions of higher and lower sensitivity of the surface coil.

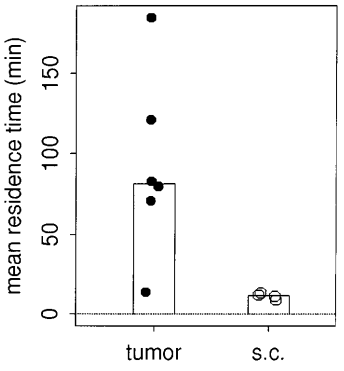

Fig. 5 Estimated mean residence time (MRT) of floxuridine at the site of injection, all experiments (*Bars* Median MRT)

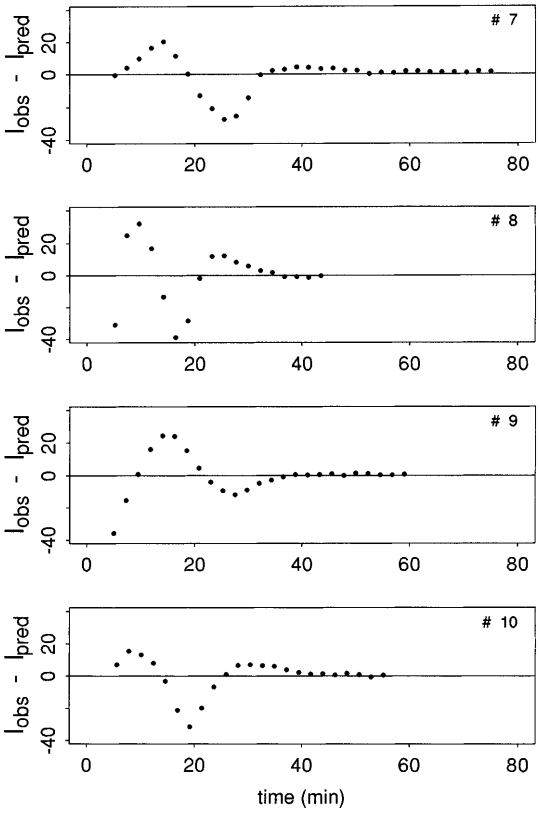

Fig. 6 In vivo [^{19}F]-NMR signal of floxuridine after s.c. injection of 30 μmol floxuridine: residuals from a fitted monoexponential disposition curve versus time after injection (I_{obs} Observed signal intensity, I_{pred} signal intensity as predicted by the monoexponential disposition model)

Discussion

The results of this study show highly variable drug disposition from tumors after local administration as opposed to rapid drug clearance with low variability from the s.c. injection site. The majority of tumors exhibited two-compartmental kinetics for floxuridine; at least a fraction of the dose (≥20%) left the tumor slowly, i.e., with a local half-life in excess of 0.5 h (up to 6 h) The signal intensity for a given amount of drug was about 1 order of magnitude lower for tumors than for the s.c. injection site.

The kinetic model used in this study (Fig. 1) is a descriptive, highly simplified model that was employed mainly to allow calculation of the MRT of the parent drug at the site of administration and the fraction converted intratumorally to FU. This model neglects floxuridine in the circulation as well as FU formed elsewhere in the body (e.g., in the liver) because upon systemic administration, floxuridine is quickly converted to FU [52], whereas FU is cleared from the blood so rapidly (half-life 15 min [3]) that it is unlikely that, at any time, appreciable amounts of floxuridine or FU would build up in the circulation from floxuridine gradually leaking from the intratumoral administration site. The model also does not distinguish between the extracellular and intracellular fluid spaces in the tumor because the signal-time data recorded for floxuridine indicate at most two kinetic compartments with clearly different scale and

exit rate parameters, whereas only one compartment can be identified for FU (Fig. 4.) It would be plausible, then, to assume that the observed floxuridine compartments reflect well-vascularized and poorly vascularized tumor regions [21, 22], although no distinction between different FU compartments can be made on the basis of these data. Experiments involving a higher intratumoral dose of floxuridine, producing larger amounts of FU, might reveal more details about intratumoral FU kinetics. The model also relies on the assumption that the ratio of the signals from equimolar amounts of floxuridine and FU is the same in vivo as that determined in vitro, which would have to be verified by additional animal experiments if an unbiased estimate of the fraction of the dose converted to FU is needed.

The long local half-life of FU (Table 1) indicates intratumoral "trapping" [53]. Intratumoral catabolism of FU must have been slow since the major catabolite, α-fluoro-β-alanine (FBAL), was found only in late sum spectra obtained from three of six tumors. (Even this small amount of FBAL might have been formed from FU in the liver and then entered the tumor from the circulation.) This is in line with the known low activity of pyrimidine catabolism in the M3924A tumor, which is one of the more rapidly growing Morris hepatomas [51]. No significant FU nucleotide signal was found in any of the spectra, including sum spectra obtained at 3–4 h after injection (Fig. 3), which suggests that anabolism of floxuridine or FU was either slow or absent. As to the anabolism of FU, this can be explained by the observation that the FU concentration was low at all times; the total amount of FU present in the tumor never exceeded 2 μmol (Fig. 4). The formation of minor amounts of fluorinated nucleotides from floxuridine or FU cannot be ruled out, however, because floxuridine and FU nucleotide signals would have been difficult to resolve in the NMR spectra (Fig. 3); floxuridine: $\delta = -90.0$ ppm; FU nucleotides: $\delta = -89.1$ to -89.2 ppm [1]. Analyses of tissue extracts would probably provide a more definite answer to the question as to whether this tumor anabolizes floxuridine or FU; they could also show anabolites that might be incorporated into RNA or DNA or be bound to thymidylate synthase.

Linear two-compartment models have been used to describe the disposition of phenol red from the tissue-isolated rat Walker 256 carcinoma after intratumoral injection [46], the residence time distribution of deuterated water (D_2O) in the tissue-isolated rat mammary adenocarcinoma R3230AC after intraarterial injection [14], and the intratumoral concentration-time course of the NMR contrast agent gadopentetate in human mammary carcinomas and fibroadenomas after i.v. injection [42]. This heterogeneity of intratumoral pharmacokinetics has been attributed to the existence of well-perfused and poorly perfused regions within solid malignant tumors [13, 18, 22]. The fast and slow disposition rate constants in our tumors with biexponential drug disposition (Table 1, tumors 1, 3, 4, and 6) differed by about 1 order of magnitude; the same difference has been observed between the fast and slow exit rate constants of D_2O in the rat mammary adenocarcinoma R3230AC [14]. All of these data suggest that many solid malignant tumors contain regions where drug exchange between blood and tissue is rather slow.

This study shows that NMR spectroscopy in vivo can be a highly effective tool in studying the local disposition kinetics of a fluorine-containing drug after intratumoral or s.c. injection. The notorious sensitivity problem of in vivo NMR is greatly alleviated in this application; with floxuridine an injected dose of only 2.5% of the reported i.p. 50% lethal dose (LD_{50}, 1,600 mg/kg [38]) is sufficient for a satisfactory characterization of local kinetics with both modes of administration. There is one report of a study where the release of FU from a gel injected into basal-cell carcinomas was monitored in a patient by [^{19}F]-NMR [54]. Subcutaneous injection experiments could be particularly useful for systematic in vivo investigations of drug release from depot preparations because, with drug solution the MRT at the site of application is short and variability is low (Fig. 5). Measurement of retardation effects upon intratumoral injection can be expected to be more difficult because in the tumors used in this study the local MRT after intratumoral administration of the drug solution was highly variable and lasted for up to several hours (Fig. 5).

Poor vascularization in parts of solid tumors can be an advantage when a drug is injected intratumorally because it will keep the drug right at the supposed site of action for a long period. The same situation is a problem when a drug is given systemically because distribution into the poorly vascularized tumor regions may not be completed before the drug concentration in the circulation falls below an effective level. Thus, there are pharmacokinetic reasons to expect that intratumoral administration of cytostatics could be a useful supplement to systemic drug administration. Successful treatments of small hepatocellular carcinomas by local ethanol injection (for a review see [6]) and of basal-cell carcinomas by local injection of an FU-containing gel [36] show that intratumoral drug application can be effective.

References

1. Arellano M, Cabanac-Longo S, Malet-Martino M, Martino R (1994) Fluorine-19 NMR is a powerful tool for discriminating the anabolites of the anticancer drug 5-fluorouracil In: Book of abstracts, 2nd annual scientific meeting of the Society of Magnetic Resonance. Society of Magnetic Resonance, Berkeley, p 1355
2. Artemov D, Bhujwalla ZM, Griffiths JR, Maxwell RJ, Judson IR, Leach MO, Glickson JD (1995) Pharmacokinetics of the ^{13}C labeled anticancer agent temozolomide detected in vivo by selective cross-polarization transfer. Magn Reson Med 34: 338–342
3. Au JLS, Walker JS, Rustum Y (1983) Pharmacokinetic studies of 5-flourouracil and 5′-deoxy-5-fluorouridine in rats. J Pharmacol Exp Ther 227: 174–180
4. Bachert P (1998) Pharmacokinetics using fluorine NMR in vivo. Prog Nucl Magn Reson Spectrosc 33: 1–56

5. Bartels M, Albert K (1995) Detection of psychoactive drugs using ^{19}F MR spectroscopy. J Neural Transm Gen Sect 99: 1–6
6. Bartolozzi C, Lencioni R (1996) Ethanol injection for the treatment of hepatic tumors. Eur Radiol 6: 682–696
7. Beal SL, Sheiner LB (eds) (1992) NONMEM User's guides. NONMEM Project Group. University of San Francisco, San Francisco
8. Becker M, Port RE, Zabel H-J, Zeller WJ, Bachert P (1998) Monitoring local disposition kinetics of carboplatin in vivo after subcutaneous injection in rats by means of ^{195}Pt NMR. J Magn Reson 133: 115–122
9. Benet LZ (1972) General treatment of linear mammillary models with elimination from any compartment as used in pharmacokinetics. J Pharm Sci 61: 536–541
10. Brix G, Bellemann, ME, Haberkorn U, Gerlach L, Bachert P, Lorenz WJ (1995) Mapping the biodistribution and catabolism of 5-fluorouracil in tumor-bearing rats by chemical-shift selective ^{19}F MR imaging. Magn Reson Med 34: 302–307
11. Brockmeier D, Ostrowski J (1985) Mean time and first-pass metabolism. Eur J Clin Pharmacol 29: 45–58
12. Buahin KG, Brem H (1995) Interstitial chemotherapy of experimental brain tumors: comparison of intratumoral injection versus polymeric controlled release. J Neurooncol 26: 103–110
13. Eskey CJ, Koretsky AP, Domach MM, Jain RK (1992) ^{2}H-Nuclear magnetic resonance imaging of tumor blood flow: spatial and temporal heterogeneity in a tissue-isolated mammary adenocarcinoma. Cancer Res 52: 6010–6019
14. Eskey CJ, Wolmark N, McDowell CL, Domach MM, Jain RK (1994) Residence time distributions of various tracers in tumors: implications for drug delivery and blood flow measurement. J Natl Cancer Inst 86: 293–299
15. Findlay MPN, Leach MO (1994) In vivo monitoring of fluoropyrimidine metabolities: magnetic resonance spectroscopy in the evaluation of 5-fluorouracil.. Anticancer Res 5: 260–280
16. Gyulai L, Wicklund SW, Greenstein R, Bauer MS, Ciccione P, Whybrow PC, Zimmerman J, Kovachich G, Alves W (1991) Measurement of tissue lithium concentration by lithium magnetic resonance spectroscopy in patients with bipolar disorder. Biol Psychiatry 29: 1161–1170
17. Haberkorn U, Krems B, Gerlach L, Bachert P, Morr I, Wiesler M, Kaick G van (1998) Assessment of glucosylifosfamide mustard biodistribution in rats with prostate adenocarcinomas by means of in vivo ^{31}P NMR and in vitro uptake experiments. Magn Reson Med 39: 754–761
18. Hamberg LM, Kristjansen PEG, Hunter GJ, Wolf GL, Jain RK (1994) Spatial heterogeneity in tumor perfusion measured with functional computed tomography at 0.05 µl resolution. Cancer Res 54: 6032–6036
19. Hashida M, Kato A, Kojima T, Muranishi S, Sezaki H, Tanigawa N, Satomura K, Hikasa Y (1981) Antitumor activity of mitomycin C-dextran conjugate against various murine tumors. Gann 72: 226–234
20. He Q, Bhujwalla ZM, Maxwell RJ, Griffiths JR, Glickson JD (1995) Proton NMR observation of the antineoplastic agent iproplatin in vivo by selective multiple quantum coherence transfer (Sel-MQC). Magn Reson Med 33: 414–416
21. Jain RK (1994) Barriers to drug delivery in solid tumors. Sci Am July: 42–49
22. Jain RK (1996) 1995 Whitaker Lecture: delivery of molecules, particles, and cells to solid tumors. Ann Biomed Eng 24: 457–473
23. Jynge P, Skjetne T, Gribbestad I, Kleinbloesem CH, Hoogkamer HFW, Antonsen O, Krane J, Bakøy OE, Furuheim KM, Nilsen OG (1990) In vivo tissue pharmacokinetics by fluorine magnetic resonance spectroscopy: a study of liver and muscle disposition of fleroxacin in humans. Clin Pharmacol Ther 48: 481–489
24. Knepp WA, Jayakrishnan A, Quigg JM, Sitren HS, Bagnall JJ, Goldberg EP (1993) Synthesis, properties, and intratumoral evaluation of mitoxantrone-loaded casein microspheres in Lewis lung carcinoma. J Pharm Pharmacol 45: 887–891
25. Komoroski RA, Newton JE, Sprigg JR, Cardwell D, Mohanakrishnan P, Karson CN (1993) In vivo ^{7}Li nuclear magnetic resonance study of lithium pharmacokinetics and chemical shift imaging in psychiatric patients. Psychiatry Res 50: 67–76
26. Kristjansen PEG, Quistorff B, Span-Thomsen M, Hansen HH (1993) Intratumoral pharmacokinetic analysis by ^{19}F-magnetic resonance spectroscopy and cytostatic in vivo activity of gemcitabine (dFdC) in two small cell lung cancer xenografts. Ann Oncol 4: 157–160
27. Kuang L, Yang DJ, Inoue T, Liu WC, Wallace S, Wright KC (1996) Percutaneous intratumoral injection of cisplatin microspheres in tumor-bearing rats to diminish acute nephrotoxicity. Anticancer Drugs 7: 220–227
28. Landrito JE, Yoshiga K, Sakurai K, Takada K (1994) Effects of intralesional injection of cisplatin dissolved in urografin and lipiodol on Ehrlich ascites tumor and normal tissues of CD-1 mice. Cancer Chemother Pharmacol 34: 323–330
29. Landrito JE, Yoshiga K, Sakurai K, Takada K (1994) Effects of intralesional injection of cisplatin on squamous cell carcinoma and normal tissue of mice. Anticancer Res 1: 113–118
30. Lockwood CG, Dob DP, Bryant DJ, Wilson JA, Sargentoni J, Sapsed-Byrne SM, Harris DN, Menon DK (1997) Magnetic resonance spectroscopy of isoflurane kinetics in humans. I. Elimination from the head. Br J Anaesth 79: 581–585
31. Lockwood CG, Dob DP, Bryant DJ, Wilson JA, Sargentoni J, Sapsed-Byrne SM, Harris DN, Menon DK (1997) Magnetic resonance spectroscopy of isoflurane kinetics in humans. II. Functional localization. Br J Anaesth 79: 586–589
32. Malet-Martino M-C, Martino R (1991) Uses and limitations of nuclear magnetic resonance (NMR) spectroscopy in clinical pharmacokinetics. Clin Pharmacokinet 20: 337–349
33. Maxwell RJ (1993) New techniques in the pharmacokinetic analysis of cancer drugs. III. Nuclear magnetic resonance. Cancer Surv 17: 415–423
34. Maxwell RJ, Frenkel TA, Newell DR, Bauer C, Griffiths JR (1991) ^{19}F-Nuclear magnetic resonance imaging of drug distribution in vivo: the disposition of an antifolate anticancer drug in mice. Magn Reson Med 17: 189–196
35. Menei P, Boisdron-Celle M, Croue A, Guy G, Benoit JP (1996) Effect of stereotactic implantation of biodegradable 5-fluorouracil loaded microspheres in healthy and C6 glioma-bearing rats. Neurosurgery 39: 117–124
36. Miller BH, Shavin JS, Cognetta A, Taylor RJ, Salasche S, Korey A, Orenberg EK, (1997) Nonsurgical treatment of basal cell carcinoma with intralesional 5-fluorouracil/epinephrine injected gel. J Am Acad Dermatol 36: 72–77
37. Nakashima E, Benet LZ (1988) General treatment of mean residence time, clearance, and volume parameters in linear mammillary models with elimination from any compartment. J Pharmacokinet Biopharm 16: 475–492
38. National Institute for Occupational Health and Safety (NIOSH) (1998) Registry of toxic effects of chemical substances (RTECS). NIOSH, Fredericksburg, Maryland
39. Newell DR, Maxwell RJ, Bisset GMF, Jodrell DI, Griffiths JR (1990) Pharmacokinetic studies with the antifolate C^2-desamino-C^2-methyl-N^{10}-propargyl-2′-trifluoromethyl-5, 8-dideazafolic acid (CB3988) in mice and rats using in vivo ^{19}F-NMR spectroscopy. Br J Cancer 62: 766–772
40. Newell DR, Maxwell RJ, Golding BT (1992) In vivo and ex vivo magnetic resonance spectroscopy as applied to pharmacokinetic studies with anticancer agents: a review. NMR Biomed 5: 273–278
41. Penn RD, Kroin JS, Harris JE, Chiu KM, Braun DP (1983) Chronic intratumoral chemotherapy of a rat tumor with cisplatin and fluorouracil. Appl Neurophysiol 46: 240–244
42. Port RE, Knopp MV, Hoffmann U, Zabel S, Brix G (1996) Pharmacokinetics of gadolinium DTPA in arterial blood and in malignant and benign mammary tumors, monitered simulataneously by dynamic NMR tomography. In: Kuhlmann J, Klotz U (eds) Clinical pharmacology and oncology (Clinical pharmacology, vol 14) W. Zuckschwerdt, Munich, pp 82–88

43. Rodrigues LM, Maxwell RJ, McSheehy PM, Pinkerton CR, Robinson SP, Stubbs M, Griffiths IR (1997) In vivo detection of ifosfamide by ^{31}P-MRS in rat tumours: increased uptake and cytotoxicity induced by carbogen breathing in GH3 prolactinomas. Br J Cancer 75: 62–68
44. Rowland M, Tozer TN (1995) Clinical pharmacokinetics: concepts and applications, 3rd ed. Williams & Wilkins. Baltimore, p 486
45. Sachs GS, Renshaw PF, Lafer B, Stoll AL, Guimaraes AR, Rosenbaum JF, Gonzalez RG (1995) Variability of brain lithium levels during maintenance treatment: a magnetic resonance spectroscopy study. Biol Psychiatry 38: 422–428
46. Saikawa A, Nomura T, Yamashita F, Takakura Y, Sezaki H, Hashida M (1996) Pharmacokinetic analysis of drug disposition after intratumoral injection in a tissue-isolated tumor perfusion system. Pharm Res 13: 1438–1444
47. Smith JP, Stock E, Orenberg EK, Yu NY, Kanekal S, Brown DM (1995) Intratumoral chemotherapy with a sustained-release drug delivery system inhibits growth of human pancreatic cancer xenografts. Anticancer Drugs 6: 717–726
48. Statistical Sciences Inc. (1992) S-Plus, version 3.1. Statistical Sciences Inc., Seattle
49. Tomita T (1991) Interstitial chemotherapy for brain tumors: review. J Neuro-oncol 10: 57–74
50. Walter KA, Tamargo RJ, Olivi A, Burger PC, Brem H (1995) Intratumoral chemotherapy. Neuro-surgery 37: 1128–1145
51. Weber G, Queener SF, Ferdinandus JA (1971) Control of gene expression in carbohydrate, pyrimidine and DNA metabolism. Adv Enzyme Regul 9: 63–95
52. Williams WM, Huang KC, Chen TS, Warren BS (1987) Dose-dependent elimination of 5-fluoro-2′-deoxyuridine in the monkey (42487). Proc Soc Exp Biol Med 184: 326–336
53. Wolf W, Presant CA, Servis KL, El-Tahtawy A, Albright MJ, Barker PB III, Ring R, Atkinson D, Ong R, King M, Singh M, Ray M, Wiseman C, Blayney D, Shani J (1990) Tumor trapping of 5-fluorouracil: in vivo ^{19}F NMR spectroscopic pharmacokinetics in tumor-bearing humans and rabbits. Proc Natl Acad Sci USA 87: 492–496
54. Wolf W, Waluch V, Kim H, Moy R, Gaudette M, Yu N, Kanekal S, Orenberg EK (1995) Noninvasive ^{19}F-magnetic resonance spectroscopy to evaluate tumoral pharmacokinetics of AccuSite (fluorouracil/epinephrine) injectable gel for treatment of human basal cell carcinoma. Proc Am Assoc Cancer Res 36: 365